Inter- and intra-annual variability of vegetation in the northern hemisphere and its association with precursory meteorological factors

Boksoon Myoung,[1] Yong-Sang Choi,[1,2,3] Seungbum Hong,[1] and Seon Ki Park[1,2,3]

Received 20 March 2012; revised 17 October 2012; accepted 20 December 2012; published 24 January 2013.

[1] Determination of phenological variation is one of the most critical challenges in dynamic vegetation modeling, given the lack of a strong theoretical framework. Previous studies generally focused on the timing of a phenological event (e.g., bud-burst or onset of growing season) and its atmospheric prompts, but not on the interactive variations across phenological stages. This study, therefore, investigated the inter- and intra-annual variability existing in all the phenological stages and the relations of the variability with four meteorological variables (surface temperature (T_s), shortwave radiation (SW), vapor pressure deficit (VPD), and precipitation ($PRCP$)) using a 25-year (1982-2006) dataset of leaf area index (LAI) from the Advanced Very High Resolution Radiometer (AVHRR). Our six study sites of each $4° \times 4°$ grids (mixed forest in China, deciduous needle-leaf forest in Siberia, evergreen needle-leaf forest in western Canada, grass in Gobi, and crops in the Central United States and southeastern Europe) include various vegetation types, local climates, and land-use types in the mid-latitudes of the northern hemisphere. Empirical orthogonal function (EOF) analysis with detrended LAI anomalies identified the two leading EOF modes that account for the amplitude and phase of the monthly LAI variations. The inter-annual correlation between the principle components (PCs) of the two modes and the meteorological variables for spring and summer showed that the amplitude and phase modes (AM and PM, respectively) were affected by different dominant meteorological factors. Over most of the study regions, AM was positively correlated with $PRCP$ and negatively with T_s, SW, and VPD, while PM was predominantly positively correlated with T_s. The contrasting responses of the two EOF modes to T_s reflect environmental limitations on plant growth such as early start of growth, but with a reduced value of maximum LAI in a year with a warm spring. In addition, insignificant correlations between AM and $PRCP$, as well as negative correlations between PM and $PRCP$, in the crop regions suggest that human interventions such as advanced irrigation systems also play a key role in vegetative activity.

Citation: Myoung, B., Y.-S. Choi, S. Hong, and S. K. Park (2013), Inter- and intra-annual variability of vegetation in the Northern Hemisphere and its association with precursory meteorological factors, *Global Biogeochem. Cycles*, *27*, 31–42, doi:10.1002/gbc.20017.

1. Introduction

[2] The terrestrial biosphere affects the atmosphere, land-surface, and climate by influencing the energy, moisture, and carbon fluxes at the surface, which in turn impact the phenology, distribution, and type of local vegetation (*Foley et al*., 1996; *Pielke et al*., 1998; *Prentice et al*., 2000; *Denman et al*., 2007). It is thus critical to understand the mechanisms behind the variations in vegetation to examine and predict not only the terrestrial ecosystems and the related carbon cycle but also the mediation of the climate system by feedbacks of the terrestrial ecosystems. Ground-based observational data sets of vegetation provided restricted usefulness for the studies and predictions of regional or global changes of vegetation due to their small spatial and temporal resolutions. Overcoming the spatio-temporal limitations of ground-based observations by using satellite-derived vegetative indices such as the leaf area index (LAI), normalized difference vegetation index (NDVI), and enhanced vegetation index (EVI) has greatly improved our understanding of the characteristics and dynamics of large scale terrestrial ecosystems (*Pettorelli et al*., 2005; *Reed et al*., 2009).

[3] Many previous studies analyzing regional and large-scale variations in vegetation found ecological responses

All supporting information may be found in the online version of this article.

[1]Center for Climate/Environment Change Prediction Research, Ewha Womans University, Seoul, Korea.
[2]Severe Storm Research Center, Ewha Womans University, Seoul, Korea.
[3]Department of Environmental Science and Engineering, Ewha Womans University, Seoul, Korea.

Corresponding author: Y.-S. Choi, New Engineering Bldg. #105-3, Ewha Womans University, Daehyun-Dong, Seodaemoon-Gu, Seoul, Korea. (ysc@ewha.ac.kr)

0886-6236/13/10.1002/gbc.20017

to environmental change (*Sharon et al*., 1990; *Richard and Poccard*, 1998; *Ichii et al*., 2002; *Wang et al*., 2003; *Nezlin et al*., 2005; Chandrasekar *et al*., 2006). These studies found responses of NDVI to temperature variability in spring and several month-lagged responses of summertime NDVI to springtime precipitation on inter-annual time scales. The former was obvious over larger areas in the mid-latitudes of the northern hemisphere, while the latter was evident only in dry regions of the subtropics and the mid-latitudes. The modulation of temperature on vegetation growth in spring was also evident over a decadal time scale; a positive long-term trend of surface temperature may cause an early increase of springtime NDVI on a regional and global scale, possibly advancing the growing season (*Piao et al*., 2003; *Studer et al*., 2005; *Jeong et al*., 2011).

[4] However, the predictability of terrestrial ecosystem models remains unsatisfactory in terms of inter- and intra-annual phenological dynamics, despite remarkable improvements in these models over the past two decades (*Myoung et al*., 2011; *Richardson et al*., 2012; references therein). This is because (1) the different physiological mechanisms of plant growth, nutrient cycling, and abiotic processes (e.g., geomorphology, soil fertility, and disturbances) may or may not be linked to atmospheric conditions, and (2) local responses to atmospheric variables vary among vegetation types (*Chandrasekar et al*., 2006).

[5] Difficulties with studying the environmental controls over plants' activities stem from several aspects of the development mechanisms of plants themselves and their environmental linkages. Generally, phenological variations of vegetation typically have four stages in the mid-latitudes (i.e., dormant, growing, mature, and senescence) that are successional and interactive with one another. For example, an earlier onset of the growing season induced by a shallower wintertime snowpack was offset by lower summertime productivity of a subalpine conifer forest due to the limited availability of water in the later growing season (*Sacks et al*., 2007; *Hu et al*., 2010). *Wang et al*. (2006) reported that enhanced vegetation activity in spring consumes moisture in soil quickly, subsequently causing drier and warmer conditions in summer over North American grasslands. This kind of vegetation feedback on the local climate may have a potential impact on vegetation development in mature and senescence stages later (*Vesala et al*., 2009; *Richardson et al*., 2010). Nevertheless, most of the previous studies using satellite vegetative indices—LAI or NDVI— have addressed vegetation variations, with a focus only on a specific season or stage (e.g., *Sharon et al*., 1990; *Richard and Poccard*, 1998; *Ichii et al*., 2002; *Wang et al*., 2003; *Nezlin et al*., 2005). Their approaches were thus limited to understanding the successional and interactive phenological variations on intra- to inter-annual time scales. Therefore, properly designed studies on the inter- and intra-annual variations across all the vegetation stages are required for a more comprehensive understanding of the plant growing mechanisms.

[6] On the other hand, the aforementioned variations in vegetation are possibly affected by different dominant meteorological factors, depending on regional climates and vegetation types. One of the difficulties of discerning the way plants respond to atmospheric conditions is attributed to the following atmospheric characteristic during warm seasons (April-October); the atmospheric conditions induced by strong atmosphere-land interactions in spring and summer are less likely to provide optimal environmental conditions for vegetation growth such as warmth, light, and moisture. For instance, dry (moist) conditions caused by rare (frequent) rainfall events tend to be associated with more (less) sunshine and/or higher (lower) air temperature. Insufficient provision of moisture, thus, renders an environment with high temperature and plenty of sunshine unfavorable for plant growth (*Hopkins*, 1999). To the contrary, moderate rainfall events lasting for a certain amount of time like a month block the light necessary for plant growth. Careful exploration of the impacts of these competitive characteristics of the atmosphere on vegetation growth is therefore crucial.

[7] In addition, the phenological variations of the vegetation of agricultural regions may have different mechanisms from those of natural vegetation regions owing to the additional effect of human interference. In particular, a negligible relationship was observed between cumulative precipitation and NDVI for crops in Greece due to systematical irrigation (*Dalezios et al*., 2002). If moisture is provided by irrigation systems over water-limited areas, the response of crops to environmental conditions will not be the same as that of natural vegetation to environmental conditions. This fact emphasizes the role of human interference in vegetative activity over cultivated vegetation regions (*Funk* and *Brown*, 2006; Brown and de Beurs, 2008).

[8] From these view points, we use empirical orthogonal function (EOF) analysis to understand intra- to inter-annual phenological variations of the mid-latitude vegetation in the northern hemisphere. We investigate major independent modes of phenological changes by integrating firstly all four stages and then the most significant meteorological factors controlling these modes. Dominant meteorological factors may differ according to the degree of human-intervention, the region and plant types. Therefore, we select six study regions with various vegetation types (e.g., evergreen and deciduous needle-leaf forests, grass, and crop), diverse local climates (e.g., warm/dry, cool/humid, and semi-arid), and different land-use types (e.g., natural vegetation and cultivated crop). In the study results, these differences among the study regions appear to project considerably diverse responses of vegetation to meteorological conditions.

2. Data and Methods

[9] Our analysis is based on the 25-year (1982–2006) LAI dataset from the Advanced Very High Resolution Radiometer (AVHRR) produced by the NASA Global Inventory Monitoring and Modeling Systems group with a spatial resolution of $1^\circ \times 1^\circ$ and a monthly temporal resolution (*Ganguly et al*., 2008). This dataset originated from the AVHRR sensors but with equivalent quality to Moderate Resolution Imaging Spectroradiometer LAI products. We chose the AVHRR dataset because of its longest period, which is crucial for the present study focusing on inter-annual variability. Furthermore, we selected LAI instead of NDVI because LAI is more directly linked to the photosynthetic rate, evapo-transpiration, and energy balance, which is required as an input for numerous ecological models (e.g., *Dickinson et al*., 1986; *Sellers et al*., 1997; *Arora*, 2002; *Quillet et al*., 2010).

[10] However, LAI data are frequently missing in many regions like outer boundaries of continents, high latitudes

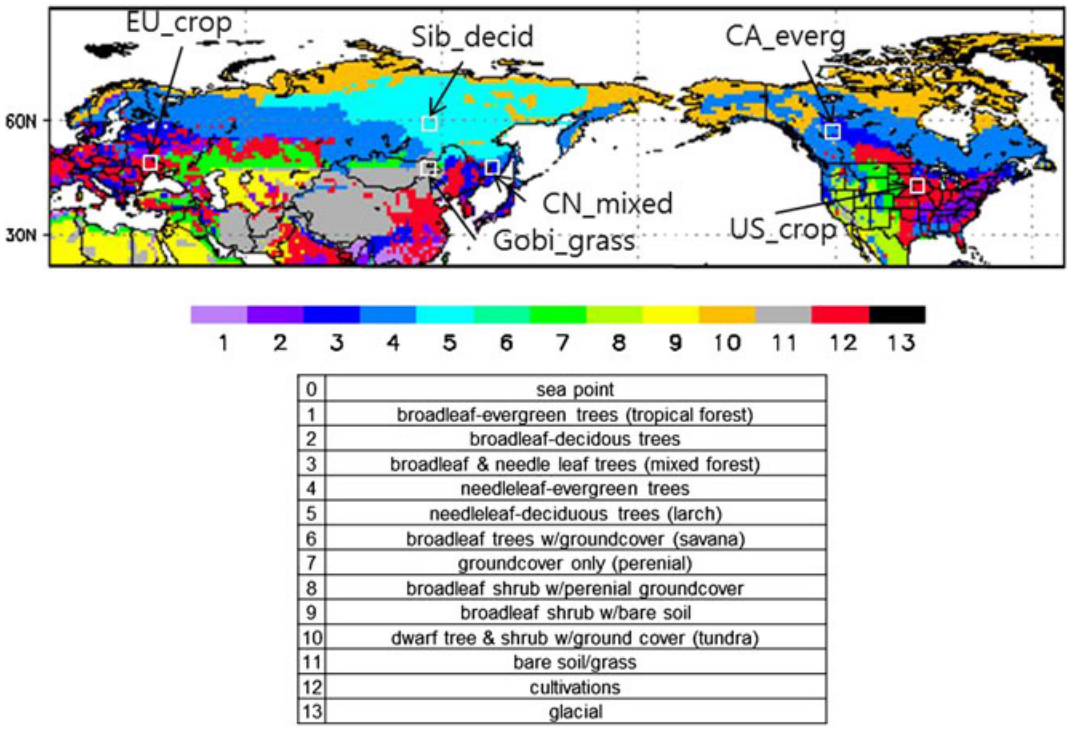

Figure 1. Map of the six study regions: a mixed forest region in north-eastern China (CN_mixed), a deciduous needle-leaf forest region in central Siberia (Sib_decid), an evergreen needle-leaf forest region in the western Canada (CA_everg), a grass region in the eastern periphery of the Gobi Desert (Gobi_grass), a crop region in the United States (US_crop), and a crop region in Europe (EU_crop). Land-use types based on NCEP land cover data set ($1° \times 1°$) are indicated with colors.

greater than 65°N, and deserts. We dealt with each $4° \times 4°$ box as the study domain between 30°N and 65°N, as shown in Figure 1. Especially, we focused on the six study regions where the LAI data cover the whole 25 years, and very diverse vegetation types, land-use types, and local climates are well characterized. The four regions (CN_mixed, Sib_decid, CA_everg, and Gobi_grass in Figure 1) are dominated by natural vegetation (natural vegetation regions, hereafter). As shown in Table 1, the land cover types are mixed forest for CN_mixed, deciduous needle-leaf forest for Sib_decid, evergreen needle-leaf forest for CA_everg, and grass for Gobi_grass under varied local climates. The two other regions are dominated by crops (US_crop and EU_crop in Figure 1) (cultivated vegetation regions, hereafter).

[11] LAIs in these sub-regions experience intrinsic inter- and intra-annual variability. Illustrated in Figure 2 is a schematic demonstrating how a phenological shape varies from year to year, compared with an average (thick solid line in Figure 2). A seasonal variation of LAI may have both (or either) higher/lower activity (thin solid lines in Figure 2) and (or) advanced or delayed development (dashed lines in Figure 2) than the average. The former variations are associated with the amplitude of the bell shaped LAI, and the latter variations with its phase. To analyze the most dominant inter-annual variability determining the shapes of LAI variations, EOF analysis was conducted. EOF analysis is an effective statistical method to identify the most extensive and influential successive patterns of data distributed in space (*Priesendorfer*, 1988). In large-scale ecological studies, this statistical method has been used to examine a spatio-temporal pattern of 2-dimensional temporal vegetation data sets and to identify major inter-annual modes that are orthogonal to and independent of each

Table 1. Information on the Locations, Types of Land Cover, and Local Climates During the Growing Season in the Six Regions Studied: A Mixed Forest Region in North-Eastern China (CN_Mixed), a Deciduous Needle-Leaf Forest Region in Central Siberia (Sib_Decid), an Evergreen Needle-Leaf Forest Region in Western Canada (CA_Everg), a Grass Region in the Eastern Periphery of the Gobi Desert (Gobi_Grass), a Crop Region in the United States (US_Crop), and a Crop Region in Europe (EU_Crop)

	Natural Vegetation Regions				Cultivated vegetation regions	
	CN_mixed	Sib_decid	CA_everg	Gobi_grass	US_crop	EU_crop
Lon/lat of the region	134-137E/47-50 N	115-118E/58-61 N	122-119 W/56-59 N	114-117E/44-47 N	96-93 W/42-45 N	28-31E/48-51 N
Land cover type	Mixed forest	Deciduous Needle-leaf	Evergreen Needle-leaf	Grass	Crop	Crop/Woodland
Climate during growing season	Warm and humid	Cool and dry	Cool and dry	Hot and very dry	Warm and dry	Warm and dry

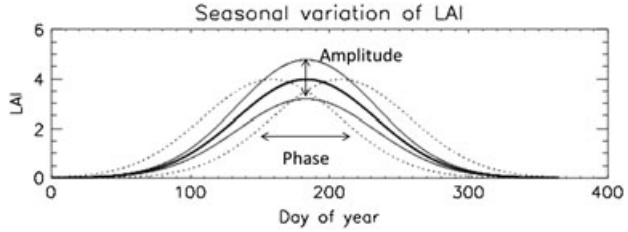

Figure 2. A schematic illustrating year-to-year variations of a phenological bell shape compared to a long-term mean (thick solid line). The shape may vary with respect to the amplitude (thin solid lines) and/or the phase (dashed lines).

other (*Sarkar and Kafatos*, 2004; *Nezlin et al*., 2005; *Studer et al*., 2005, 2007). Likewise, the EOF method can also be applied to 1-dimensional time series data sets. For instance, EOF analysis with cyclone landfall records along the west coast of the United States successfully detected dominant inter-annual variability of storm activity (Myoung and Deng, 2009). In order to capture both inter- and intra-annual variability in LAI integrating all of the phenological stages, we used EOF analysis for one-point LAI data sets.

[12] For each study region, the LAI dataset was composed of 300 (=12 (month) x 25 (years)) monthly values from 1982 – 2006 that were spatially averaged over the study region. Detailed EOF analysis includes the following procedures. i) For each study region, a 25-year monthly mean was first removed, and, subsequently, a monthly long-term trend was removed, producing monthly detrended anomalies. ii) The singular value decomposition was applied to the monthly detrended anomalies of LAI, assuming the temporal space from January to December in the LAI dataset as a spatial space (e.g., x-space). The result of EOF analysis provides 25 EOF modes and their corresponding principle components (PCs).

[13] For a correlation analysis between the PCs of the EOF modes and atmospheric conditions, four meteorological variables that are known to be essential to plant growth were considered: surface temperature (T_s), precipitation (*PRCP*), atmospheric vapor pressure deficit (*VPD*), and net shortwave radiation at surface (*SW*) (*Hopkins*, 1999; *Nemani et al*., 2003). In addition to T_s and *PRCP*, which are known to be significant atmospheric drivers for vegetation developments, *VPD* and *SW* were also included. *SW* plays a significant role in seasonal variations of Amazon rainforests (*Huete et al*., 2006; *Myneni et al*., 2007). *VPD* is useful in determining the sensitivity of vegetative activity to both moisture and temperature. The benefits of evaluating *VPD* are twofold. Firstly, it accounts for atmospheric humidity. In general, higher *VPD* indicates lower relative humidity in the atmosphere on an inter-annual time scale. Since plants close their stomata and their photosynthesis rate drops as the environmental *VPD* increases (*Grantz*, 1990; *Rastetter et al*., 1992; *Körner*, 1995; *Mu et al*., 2007), *VPD* is one of the factors limiting plant photosynthesis in non-humid areas. Secondly, during a warm season, the impact of local land-surface is more significant than that of large-scale circulations over some land areas, so that *VPD* tends to be negatively correlated with *PRCP* and soil moisture through positive feedbacks between the atmosphere and land-surface (*Koster et al*., 2004; *Myoung and Nielsen-Gammon*, 2010a, 2010b). Thus, *VPD* reflects the dependence of vegetation on not only atmospheric humidity but also moisture deficiency in soil, which is caused by prolonged *PRCP* deficits during the warm season.

[14] The meteorological variables were obtained from the monthly Global Land Data Assimilation System (GLDAS) dataset for the period corresponding to the LAI dataset. The atmospheric *VPD* was calculated from T_s, specific humidity, and pressure at the surface, while the other variables were directly obtained from the monthly GLDAS dataset. Caution should be taken when interpreting and understanding the results of the correlation analysis, in which the meteorological variables in this paper are not based on monthly averages in GLDAS. In an attempt to draw physically meaningful correlations and to avoid possible statistical artifacts, we computed averages of the meteorological variables over a period of two consecutive months between February and August (i.e., February-March, March-April, . . ., and July-August) for each region. Then, after removing long-term trends (1982-2006), we correlated the detrended two-month averages of the meteorological variables with PCs of major EOF modes (for more detailed information, see Supporting Material). The two-month averages provided more stable correlation analysis results than one-month averages, perhaps because of the exclusion of large natural variability in monthly meteorological variables.

3. Results

3.1. Dominant EOF Modes and Their Principle Components (PCs)

[15] Figure 3 presents the 25-year monthly mean of LAI with standard deviations (Figure 3a) and the two leading EOF modes (Figs. 3b and c) for each region. Although the results of EOF analysis are shown only for the six study regions here, similar EOF modes were also observed in the regions adjacent to the six regions. In Figure 3a, the phenological variation of LAI for all of the regions is bell shaped. Variations of LAI are larger when LAI is higher. Here, we defined a growing season (indicated by blue shade in Figure 3a) as the period during which an increase of LAI begins and a decrease of it ends. The periods of the growing season were April-October in CN_mixed, April-October in Sib_decid, March-November in CA_everg, May-October in Gobi_grass, April-November in UC_crop, and March-November in EU_crop. Although the growing seasons in this study were not identical to those defined in other studies such as *Jeong et al*., (2011) (due to different definitions of growing season and different resolutions of datasets), the regional variations of the onset of the growing season were roughly consistent with their results.

[16] The first mode accounted for the amplitude of LAI variations (amplitude mode, AM, hereafter), i.e., the positive (negative) value of AM indicates enhanced (degraded) vegetative activity within the growing season (Figure 3b). The maximum AM month was coincident to the month of the largest variation of LAI, which was usually the month of the highest LAI value of the 25-year mean. The period of positive AM is referred to as "intensive growing season" (indicated by the pink shade). The intensive growing season usually started one or two months later than the beginning of the growing season. Before the intensive growing season started, the AM values were negligible (CN_mixed, CA_everg, Gobi_grass, and US_crop) or slightly negative (Sib_decid

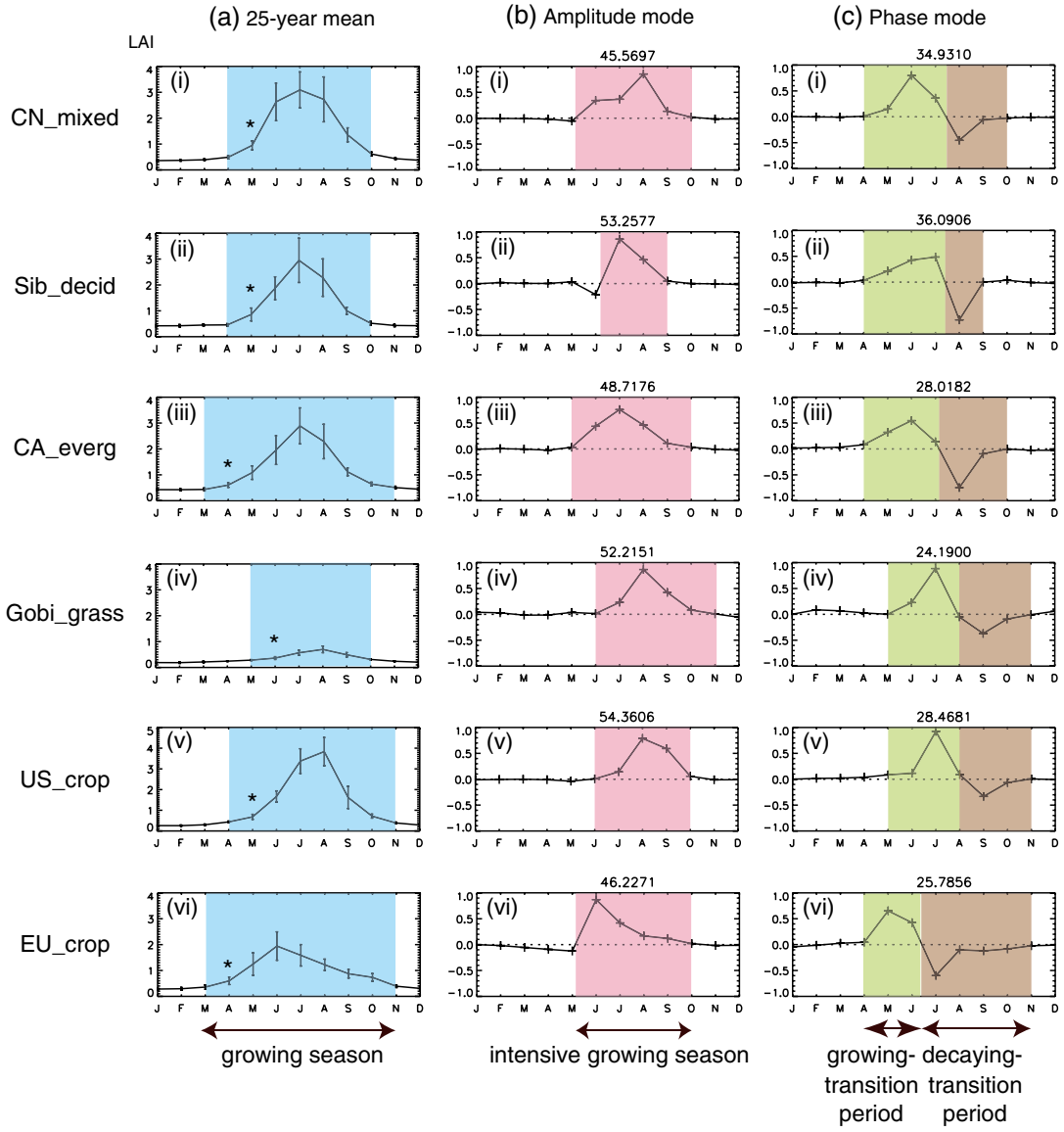

Figure 3. A 25-year mean of monthly LAI with error bars (a), the amplitude mode (AM) (b), and the phase mode (PM) (c) of the six regions in the study (i – vi). The first four regions (CN_mixed, Sib_decid, CA_everg, and Gobi_grass) are those with natural vegetation and the other two are those with cultivated vegetation. The X-axis represents the months. The numbers in the sub-title of each EOF mode indicate the percentage variability explained by the mode. The blue-shaded period in (a) and the pink-shaded period (b) refer to the newly defined growing season and the intensive growing season, respectively. Similarly, the green- and brown-shaded periods in (c) indicate the growing- and decaying-transition periods, respectively. Stars in (a) indicate the "yardstick" month for inter-annual variations of the start of the growing season (for more detail, see the text).

and EU_crop), which implied that LAI variations in the very early growing season (e.g., onset of a growing season) were probably unrelated with those in the intensive growing season.

[17] The second mode (Figure 3c) exhibited a dipole structure mainly before and after the peak period of the 25-year mean LAI. This mode accounted for the phase shift of LAI maximum (phase mode, PM, hereafter) because when the PM values are added to the 25-year averages, the phase and timing of the maximum LAI are shifted forward (positive PM) or backward (negative PM) depending on signs of PM, as illustrated by the skewed dashed lines of the schematic in Figure 2. The periods with positive and negative values generally corresponded to the transition periods from dormant to mature stages and from mature to dormant stages, respectively. Thus, the positive periods are referred to as the "growing-transition period" (the green shade), and the negative periods as the "decaying-transition period" (the brown shade).

[18] During the years with a strong PM phase but negligible AM phase, the signs of LAI anomalies between the two transition periods can be the opposite. In order to examine the frequency of occurrence of this "seesaw" pattern in each region, we computed the turnover rate (Table 2). This turnover rate is defined as the proportion of years in which the sign of the LAI anomaly averaged over the growing-transition period is different from that averaged over the decaying-transition

Table 2. Turnover Rate (%)Defined as the Proportion of the Number of Years When a Sign of the Mean LAI Anomaly During the Growing-Transition Period Is Opposite to That During the Decaying-Transition Period out of the 25 Years for Each Study Region

	Turnover rate (%)
CN_mixed	48
Sib_decid	56
CA_everg	48
Gobi_grass	56
US_crop	56
EU_crop	36
Average of the six regions	50

period, out of the 25 years. The average turnover rate of 50% for all the regions implies that PM exerted a considerable influence on LAI, despite being the second dominant mode.

[19] To determine whether a positive (negative) PM phase implies an advanced (delayed) start of a growing season in a particular year, we assumed that LAI values in a specific month indicated by the star in (i)-(iv) of Figure 3a were a reasonable yardstick to measure the inter-annual variability of the start of the growing season, and then computed the correlation coefficient between the PC of PM and the LAI anomalies in the yardstick month. Significant positive correlations at the 99% confidence level, ranging from 0.45 to 0.76, were found in most of the regions except EU_crop. This suggests that positive (negative) PM generally indicates an advanced (delayed) start of the growing season.

[20] The AM and PM explained approximately 72–89% of the total variance (from 72% for EU_crop to 89% for Sib_decid). They were also identified at the $1^\circ \times 1^\circ$ resolution, but not in every grid, because LAIs at the $1^\circ \times 1^\circ$ resolution were highly variable. At the spatial scale greater than the 4° 4° resolution, PM became vague while AM remained prominent. It was presumed that excessive spatial averages tended to remove local characteristics responsible for PM. For these reasons, AM and PM were the most robust at the $4^\circ \times 4^\circ$ resolution.

[21] The PC time series of AM and PM (PC_AM and PC_PM, respectively) are displayed in Figs. 4a and b, respectively. In order to examine the dominant role of AM in determining the amplitude of LAI variations, we performed a composite analysis of the top five positive and negative PC_AM years out of the total 25 years, denoted by diamonds and triangles in Figure 4a, respectively. According to Table 3, during the intensive growing season, the mean LAI values of the top five positive years were significantly higher than those of the top five negative years in all the study regions at the 95% level. This result confirmed that AM dominantly controlled the LAI amplitude during the warm season.

[22] Figure 4 also show different characteristics of inter-annual variations of the PC time series of the two modes that are dependent on regions. In particular, the magnitude of the EOF modes was substantially reduced from about 2000, mainly over the natural vegetation regions. At the higher latitudes (i.e., Sib_decid and CA_everg), this characteristic was observed in both PC_AM ((ii) and (iii) in Figure 4a) and PC_PM ((ii) and (iii) in Figure 4b). This may have been associated with various factors such as meteorological conditions, vegetation types, and the degree of human interference. In the following subsection, we explore how these factors affect vegetation activity on an inter-annual time scale in terms of PCs of the EOF modes of LAI.

3.2. Correlation Analysis

[23] Meteorological factors may control AM and/or PM throughout a year. Finding EOF modes of monthly meteorological variables (T_s, *SW*, *PRCP*, and *VPD*) for which PCs are highly correlated with PC_AM or PC_PM may indicate that the meteorological variables control plants throughout a year. However, we could not find such EOF modes having statistically meaningful correlations. Instead, based on the expectation that atmospheric conditions during a specific period influence the EOF modes of LAI, we correlated the meteorological data averaged over 2 consecutive months (within the period of February to July) with PC_AM or PC_PM.

[24] Figure 5 shows the highest correlation coefficient (color bars) for AM (a) and PM (b). The corresponding 2 months over which meteorological data were taken are shown as characters at the end of each color bar for each region (the complete results are shown in Tables 1 and 2 of Supporting Material). In Figs. 5a and 5b, the months of the intensive growing season and the growing-transition period are also indicated below the names of the regions, respectively. The intensive growing season (growing-transition period) starts between June and July (May and July). In order to understand the influence of 'preceding' atmospheric conditions on PCs, the meteorological variables for February-March, March-April,. . ., and lastly for the first two months of the intensive growing season (growing-transition period) were only considered, when selecting the 2 months of the highest correlation. Note that correlation coefficients between *VPD* and PCs (at the end of each color bar in Figure 5) are what are multiplied by –1.0 in order to enable a comparison with the correlations of *PRCP*.

3.2.1. The Amplitude Mode (AM) of LAI

[25] According to Figure 5a, PC_AM was positively correlated with *PRCP* in the natural vegetation regions. This positive sign of the correlation was not statistically significant at the 95% confidence level in CN_mixed and CA_everg, but it was observed with no exceptions in all of the four natural vegetation regions. The PC_AM's positive correlations with *PRCP* were consistent with the previous finding that more springtime rainfall than average is favorable for greener conditions in the subsequent summer over the inner-continental regions of the mid-latitudes (*Ichii et al*., 2002; *Wang et al*., 2003; *Nezlin et al*., 2005). On the other hand, in the cultivated vegetation regions, these correlations were negligible and even negative in the US_crop region. Variations of springtime *PRCP* did not seem to be responsible for the variations in AM in these regions, which could be attributed to sufficient water supply through well-developed irrigation systems in the croplands.

[26] In addition to *PRCP*, this study identified the negative correlations of PC_AM and T_s, and of PC_AM and *SW* in both the natural and cultivated vegetation regions. These two meteorological variables had generally stronger correlations with PC_AM than *PRCP* had. Negligible correlations between *PRCP*, T_s, and *SW* (not shown) during the months

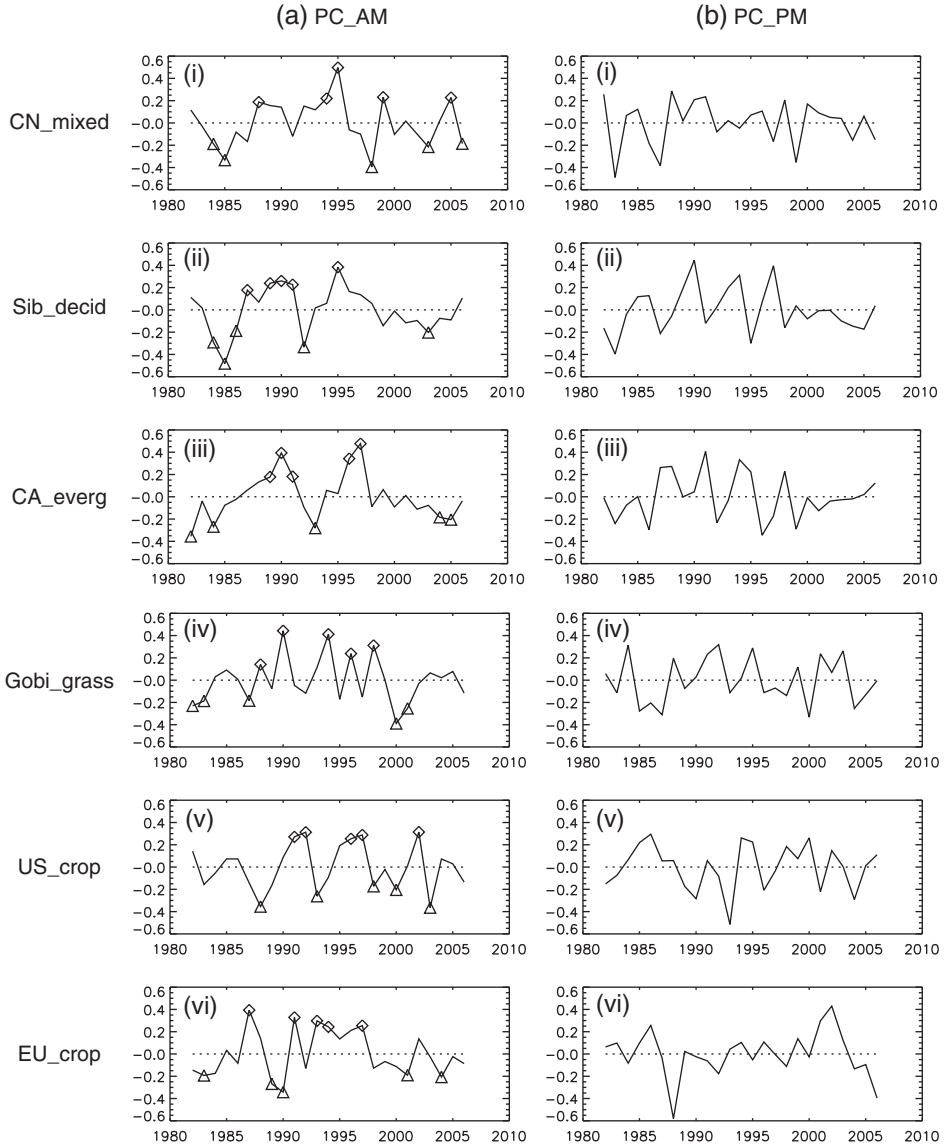

Figure 4. Principle components (PCs) of the amplitude mode (PC_AM) (a) and the phase mode (PC_PM) (b) in the six study regions (i – vi). The abscissa represents years from 1982 to 2006. In (a), diamonds (◊) and triangles (Δ) indicate the top five positive and negative AM years, respectively.

of the highest correlation described in Figure 5a imply that the correlations between PC_AM and T_s and between PC_AM and *SW* did not come from the correlation between PC_AM and *PRCP*.

Table 3. Mean LAI During the Intensive Growing Season Between the Top Five Positive and Negative PC_AM Years and Differences in Each Study Region

	Top five positive years	Top five negative years	Difference
CN_mixed	2.89	1.97	1.10 (46.7%)
Sib_decid	3.46	1.88	1.63 (84.0%)
CA_everg	2.60	1.66	0.28 (56.6%)
Gobi_grass	1.37	1.01	0.33 (35.6%)
US_crop	3.54	2.54	1.25 (39.4%)
EU_crop	1.73	1.13	0.60 (53.1%)

[27] The simultaneous correlations between PC_AM and *PRCP* (positively) and between PC_AM and T_s (negatively) in the natural vegetation regions suggest that rainy and cool environments in spring or early summer were also favorable for higher vegetation production in the intensive growing season. This result is consistent with the negative correlations between PC_AM and *VPD*, as represented in Figure 5a, i.e., low *VPD* (cooler and moister atmosphere) associated with high PC_AM. This negative relationship was statistically significant at the 95% level for both natural and cultivated vegetation except in CN_mixed ($p\_value = 0.09$ in CN_mixed). For the cultivated vegetation regions, the linkage with *PRCP* was weaker than in the natural vegetation regions; the correlation of PC_AM and *PRCP* was even negative in the US_crop region. Nevertheless, PC_AM and *VPD* were strongly correlated, which implies that the photosynthetic rates of vegetation remain

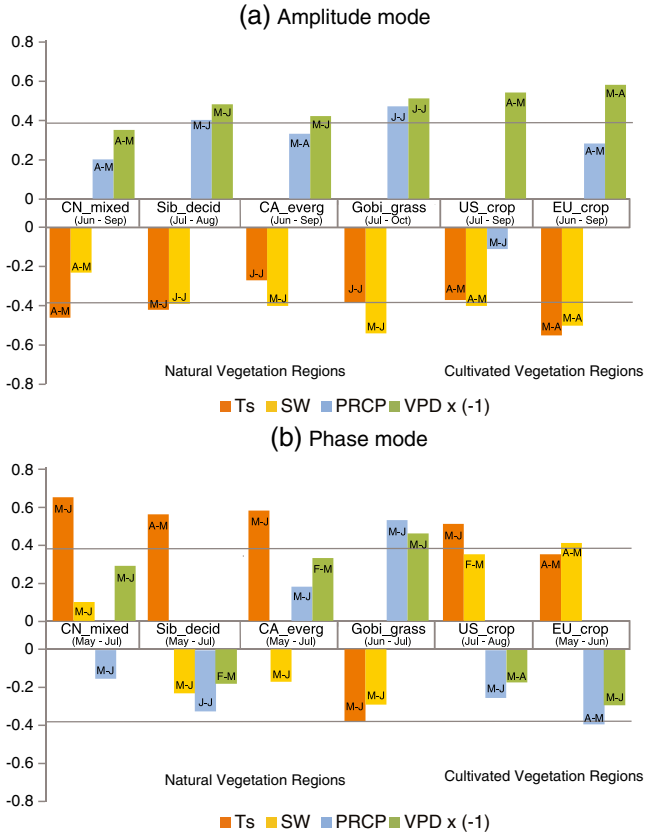

Figure 5. Correlation coefficients (r) of the four meteorological variables with the principle component (PC) of the amplitude mode (PC_AM) (a) and the phase mode (PC_PM) (b) in each study region. T_s, *SW*, *PRCP*, and *VPD* refer to two-month averaged 2-m temperature, short-wave radiation at surface, precipitation, and vapor pressure deficit, respectively. Note that the correlation coefficients of PCs with *VPD* were multiplied by (−1.0) to make it easy to compare these with those with *PRCP*. Characters specified at the end of the color bars indicate the period in which the highest correlation occurs, as follows: F-M (February and March), M-A (March and April), A-M (April and May), M-J (May and June), and J-J (June and July). (The period is not a single month but two months since T_s, *SW*, *PRCP*, *and VPD* are the average values for two consecutive months.) The months of the intensive growing season and the growing-transition period defined in Figure 3 are also shown below the names of the study regions in (a) and (b), respectively. Gray lines indicate the 95% confidence level.

dependent on *VPD* in crop dominant regions, as long as sufficient water is provided by the advanced irrigation systems in the croplands.

[28] Although previous studies seeking the association between atmospheric conditions and vegetation indices on large spatial scales mainly focused on meteorological factors such as *PRCP* and temperature, several studies discovered close links between plant growth and *VPD* in the croplands of semi-arid Africa (*Funk and Brown*, 2006; *Brown and de Beurs*, 2008). Their linkage seems to be observed in the mid-latitudes. In this study, the correlations between PC_AM and *VPD* were stronger than those between PC_AM and T_s and between PC_AM and *PRCP* in most of the regions except CA_everg. In addition, the sign and strength of the correlation between PC_AM and *VPD* did not change abruptly for the following several months after the month of the highest correlation for *VPD* in the crop-dominated regions (refer to Tables 1 and 2 in Supporting Material). This occurred despite the substantially reduced correlations with *PRCP* and with T_s in those periods.

[29] The closer connection of PC_AM to *VPD* than to *PRCP* or T_s may have been associated with the characteristics of *VPD* or their combination as follows. Firstly, the photosynthetic rate of plants responds to the environmental *VPD* negatively (direct effect) through stomata opening and closing. This response occurs on a short time scale of less than an hour (*Grantz*, 1990; *Rastetter et al*., 1992; *Körner*, 1995), but may lead to a negative relationship between *VPD* and vegetative productivity on a longer time scale like a month. Secondly, atmospheric *VPD* represents plant water stress integrated in both soil and atmosphere on a time scale longer than a month (indirect effect). *Mu et al*. (2007) emphasized that inter-annual variability of water stress is determined solely by atmospheric *VPD* in most regions of China and the US, instead of a combined water stress estimate derived from the soil/leaf and the atmosphere. An estimation of a plant's water stress by atmospheric *VPD* is partly due to the feedbacks of soil moisture to the atmosphere. During a warm season, these feedbacks occur vigorously over some land areas in which the impact of local land-surfaces is more significant than that of large-scale

circulations (*Koster et al*., 2004; *Myoung and Nielson-Gammon*, 2010a, 2010b). In addition, since *VPD* is also sensitive to moisture externally transported from other regions such as adjacent oceans, in addition to moisture locally provided from the land-surface (e.g., evapotranspiration), *VPD* successfully demonstrates water stress in the atmosphere on vegetation activity. Detailed explanations for the relationship between springtime *VPD* and plant growth in the growing season are beyond the scope of this study. However, the strong correlation between PC_AM and *VPD* across all the study regions, including US_crop and EU_crop, suggests a possible connection between *VPD* in the early growing season (March-July) and plant growth rates in the subsequent stage.

3.2.2. The Phase Mode (PM) of LAI

[30] The correlation patterns of PC_PM with the meteorological variables were more complicated than those of PC_AM (Figure 5b). Nevertheless, strong positive correlations were observed with T_s over the natural and cultivated vegetation regions except the Gobi_grass region. They were statistically significant at the 95% level except in EU_crop ($p\_value = 0.09$ in EU_crop). This strong sensitivity to temperature indicates that plants grow fast in years with warm springs. In general, except for US_crop region, the temporal gap between the first month of the highest correlation with T_s and the first month of the growing-transition period for PM was one month or shorter than that (Figure 5b), while the gap between the first month of the highest correlation with *VPD* and the first month of the intensive growing season for AM was 1–3 months (Figure 5a). This implies that PM responds to T_s more quickly than does AM to *VPD*.

[31] In Figure 5b, for the natural vegetation regions such as CN_mixed, Sib_decid, and CA_everg, more rainfall, higher humidity, and an abundant amount of radiation did not seem to contribute to greener environments in the growing-transition period (negligible correlations of PC_PM with *PRCP*, *VPD*, or *SW*). No specific directions in the correlation of PM with *SW*, *PRCP*, or *VPD* among these regions were found, which contradicts the coherent directions of the correlations of AM in Figure 5a. Radiation does not have a significant positive impact on vegetation activity in the natural vegetation regions, while it plays a significant role in the seasonal variation of vegetation activity in tropical forests such as the Amazon (*Nemani, et al*., 2003; *Huete et al*., 2006; *Myneni et al*., 2007). In contrast, temperature hardly limits plant growth in the tropics but is crucial to the early growing season's development of plants in the extra-tropics (*Nemani et al*., 2003). This feature is more pronounced in the regions of Sib_decid and CA_everg, which are located at higher latitudes than the other four study regions.

[32] On the other hand, for the cultivated vegetation regions, PC_PM was positively correlated with *VPD* and *SW*, and negatively with *PRCP*. This correlation pattern reversely paralleled that for PC_AM and the meteorological variables (Figure 5a) for the cultivated vegetation regions especially EU_crop (i.e., the positive correlation with *PRCP* and the negative correlations with T_s, *SW*, and *VPD*). This combination of correlations is indicative that crops grow more actively during the growing-transition period when in warm and dry environments with little *PRCP* and plenty of sunlight. If irrigation systems ensure sufficient water supply for crop-growth, enhanced crop-growth in late spring may be achieved even under a drought-like condition (not a real agricultural drought condition) with plenty of sunlight. Frequent occurrences of rainfall, in other words, imply reduced sunlight and air temperature, which can adversely affect vegetation growth. This speculation is supported by the positive relationships of PC_PM with T_s and *SW* in both US_crop (r[PC_PM, T_s] = 0.51 and r[PC_PM, SW] = 0.35) and EU_crop (r[PC_PM, T_s] = 0.35 and r[(PC_PM, SW] = 0.41).

[33] Lastly, in the semi-arid Gobi_grass region, water stress was the most important limiting factor for both PM and AM, which is supported by the inverse correlations of PC_PM with T_s and *PRCP* (r[PC_PM, T_s] = -0.38 and r[PC_PM, *PRCP*] = 0.53) and the negative correlation of PC_PM with *VPD* (r[PC_PM, *VPD*] = -0.46). According to Figure 5, the positive phase of AM and PM tends to be induced by more precipitation and humid conditions in May-June and in June-July, respectively.

3.2.3. Conflict Between the Amplitude and Phase Modes (AM and PM) of LAI

[34] One of the interesting results from Figure 5 is the opposite responses of AM and PM to T_s. The negative correlation of PC_AM and T_s should be understood in association with humidity. For example, colder and moister conditions, both of which lead to lower *VPD* in spring or early summer, may enhance vegetation activity. For PM, however, it is clear that warmer conditions tend to induce higher LAI in the growing-transition period (except Gobi_grass).

[35] In order to explain how these two features jointly contribute to LAI variations, Figure 6 illustrates the influential months (i.e., correlations significant at the 90% confidence level) for AM by *VPD* (dark arrows) and those for PM by T_s (white arrows), based on the complete results of the correlation analysis (Tables 1 and 2 in Supporting Material). The negative correlations of both AM and PM with T_s led to the exclusion of Gobi_grass region from Figure 6. In Sib_decid and CA_everg, the beginning of the influential months for PM by T_s preceded those for AM by *VPD*. Accordingly, over these regions, AM and PM can be simultaneously in positive phases within a year (i.e., enhanced vegetation activity from spring through summer), when some ideal circumstances occur such as i) warmer environment in early spring and ii) cooler and damper environment associated with higher precipitation in the following late spring or early summer. Due to the cold climates in Sib_decid and CA_everg at the higher latitude, a sufficient amount of sunlight and warm temperature as in the former circumstance act as essential conditions for plant growth first, after which

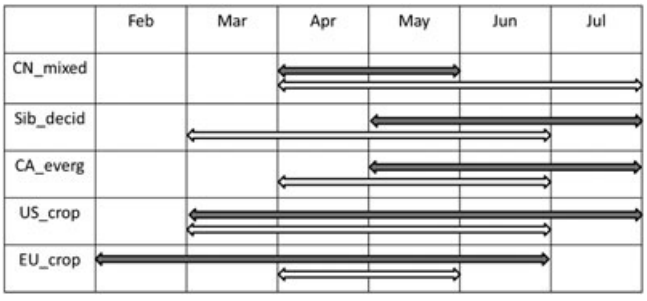

Figure 6. The periods when the AM-*VPD* (dark arrows) and PM-T_s (white arrows) correlations are significant at the 90% confidence level.

the humid conditions as in the latter circumstance enhance vegetation growth in the intensive growing season. This combination of atmospheric conditions could eventually increase the productivity of plants.

[36] However, an anomalous temperature tendency often lasts for several months during the early growing season. In this season, the strong dependency of relative humidity to thermal conditions is likely to cause positive correlations between *VPD* and T_s, as observed in this study (Table 4), indicating that warm months tend to be dry. Meanwhile, the influential months for AM by *VPD* and the influential months for PM by T_s overlapped each other at least for two months (April-May for CN_mixed, May-June for Sib_decid and CA_everg, March-June for US_crop, and April-May for EU_crop). In most of these overlapped influential months, the positive correlations between *VPD* and T_s were statistically significant at the 95% level (Table 4). Under these circumstances, the same phases for AM and PM are less likely to occur in a year, in particular because the same phases of AM and PM prefer contradictory preceding atmospheric conditions (e.g., low *VPD* for positive AM and high T_s for positive PM), while *VPD* and T_s are positively coupled in nature.

[37] To test the compatibility of the two EOF modes of LAI, we selected the years when the absolute magnitude of either PC_AM or PC_PM was greater than one standard deviation of PC_AM and PC_PM ($\sigma = 0.203$) in each region. This selection was made under the assumption that a tendency of the combination of AM and PM is more pronounced during years with substantially strong phases of the EOF modes than during their neutral years. Among these years, we computed the proportion of the years in which AM and PM have the same signs and their absolute magnitudes are both greater than σ. The proportion was small (ranging from 0% to 8%), supporting the notion that a strong positive (negative) phase of AM rarely accompanies a strong positive (negative) phase of PM. This result was attributed to the contrasting responses of AM and PM to the atmospheric thermal condition. These characteristics of AM and PM may explain the identification of AM and PM as two independent leading EOF modes in this study, which implies environmental limitations on plant growth (e.g., advanced start of growing but low amplitude of LAI in a year with a warm spring).

4. Discussion and Conclusion

[38] This study investigated the inter- and intra-annual variability in plant phenology using satellite-derived LAI from 1982 to 2006 in six regions located in the northern hemisphere. The EOF analysis with one-point monthly LAI dataset successfully identified two major independent modes (AM and PM) that integrate all the stages and are influenced by different atmospheric drivers. The AM mode as a monopole structure was associated with the amplitude of the LAI variations, especially during the intensive growing season. The PM mode was responsible for the LAI variations before and after maximum LAI (i.e., the growing- and decaying-transition period). Especially for PM, the advanced (delayed) development of vegetation during the growing-transition period was offset by advanced (delayed) decay during the decaying-transition period, thus reducing the inter-annual variations of annually integrated LAI values. Explanations for this seesaw variation in LAI remained unclear, because our correlation analysis focused on the meteorological factors contributing to plant development during spring and summer seasons only. It could be attributed to interaction between vegetation and environmental conditions (e.g., *Wang et al*., 2006; *Sacks et al*., 2007; *Hu et al*., 2010), physiological constraints for plant growth (e.g., leaf aging), varied responses of diverse plant species within the study region, or a combination of these factors (e.g., *Richardson et al*., 2010). Identifying the mechanisms underlying the seesaw pattern of LAI is a promising avenue of investigation for future studies.

[39] The effects of meteorological conditions on leaf activity were investigated through correlation analysis between meteorological data in early growing seasons and the PCs of the two modes. The correlation results for AM indicate that the overall cool and moist conditions of spring or early summer lead to enhanced photosynthetic rates and higher LAI during the intensive growing season. In the case of PM, although the influences of meteorological variables are more complicated, it was generally found that a warmer condition advances vegetation growth for all of the study regions except Gobi_grass, where a wetter environment produces the advanced development. However, a warmer and drier atmosphere with lower precipitation seems to be favorable for enhanced crop growth in US_crop and EU_crop. Of course, these correlation analyses do not verify any causality between two variables, and the effects of "third variables' that may have mediated between the two variables cannot be ruled out. Nevertheless, our results of correlation analysis do not contradict those of the previous studies that focused on specific stages of a phenological cycle (*Sharon et al*., 1990; *Richard and Poccard*, 1998; *Ichii et al*., 2002; *Wang et al*., 2003), in terms of the linkages between springtime precipitation and summertime vegetation activity or the linkages between springtime temperature and springtime vegetation activity. The former linkage was confirmed by the positive correlations between PC_AM and *PRCP* across the natural vegetation regions, as shown in Figure 5a. The latter linkage was confirmed by the positive correlations between PC_PM and T_s in most of the study regions, as shown in Figure 5b.

[40] This study has shed light on several interesting characteristics of vegetation growth in the mid-latitude. One characteristic is the positive and negative correlations of AM and PM with temperature, respectively. This contrasting correlation pattern is indicative that meteorological conditions preferred by an advanced development of vegetation in spring and advanced decay in fall are less likely to cause a greener

Table 4. Correlation Coefficients Between T_s and *VPD* During the Early Growing Season (March-June)

	March and April	April and May	May and June
CN_mixed	0.42[a]	0.35[b]	0.28
Sib_decid	–0.31	0.21	0.56[a,b]
CA_everg	0.48[a]	0.51[a]	0.38[b]
US_crop	0.71[a,b]	0.69[a,b]	0.61[a,b]
EU_crop	0.55[a]	0.39[a,b]	0.21

[a]Significant at the 95% confidence level.
[b]The correlation for the period when both AM-*VPD* and PM-T_s correlations are significant.

summer, thereby causing less pronounced relationships of plant productivity between spring and summer (e.g., *Richardson et al*., 2010). This result implies that plant productivity will be restrictive in the future unless warming climates are accompanied by moistening. Another interesting finding is that *VPD* is a significant factor for AM, regardless of regions with natural or cultivated vegetation. Correlations between *VPD* and PC_AM were higher than those between *PRCP* and PC_AM and between T_s and PC_AM. This is because plants' photosynthesis rates drop when the environmental *VPD* increases substantially (direct effect) and/or because *VPD* represents plant water stress integrated in both soil and atmosphere on a time scale longer than a month (indirect effect). In regions with cultivated vegetation, *VPD* considerably influences PC_AM, despite low correlations of PC_AM and *PRCP*. These results emphasize the direct and/or indirect effects of *VPD* on vegetative activity.

[41] In addition, the dominant meteorological factors controlling plants' activity are substantially influenced by human intervention. In this study, we identified the variation of the characteristics in plant responses to environmental conditions between the natural and cultivated vegetation regions. In contrast to the strong positive correlation between *PRCP* and PC_AM in natural vegetation regions (Figure 5a), the absence of strong positive correlations between *PRCP* and PCs (both PC_AM and PC_PM) in cultivated vegetation regions (Figs. 5a and b) can be explained by the sufficient soil moisture maintenance provided by well-developed irrigation systems. For crops, rather than *PRCP* variations, the variations in *VPD* and temperature/radiation seem to play a critical role in the variations of PC_AM and PC_PM, respectively. This suggests that human intervention plays a key role in the phenological activity of vegetation across the cultivated vegetation regions, just as the influence of atmospheric conditions is important.

[42] One of the drawbacks of this study is the limited coverage of the study regions, which mainly focused on the interior regions of the northern hemisphere, due to the frequent missing data sets of LAI near the oceans. This is possibly associated with the strong dependency of PC_AM on *PRCP* and *VPD* (Figure 5a) in our study regions in the mid-latitudes. In humid regions, the temperature and/or availability of sunlight may be important factor(s) for plant growth, due to the abundant moisture supply from the oceans through local or large-scale circulations (e.g., *Huete et al*., 2006; *Myneni et al*., 2007). This feature may be responsible for the less pronounced correlation between PC_AM and *VPD* in this study for CN_mixed (Figure 5a), which is located close to the Pacific, compared to the other regions. The application of EOF analysis to other regions such as tropical forests and dry regions is expected to reveal unique regional characteristics of the vegetation responses to atmospheric conditions. In addition, the study results provide limited information about the plant's activity during the periods of the spring onset and autumn senescence, owing to the low temporal resolution of the dataset used in this study and the negligible LAI variability in the very early and late growing season compared to that in the active growing season (Figure 3a). More suitable datasets and analysis methods are required to reveal the connections between the timing of onset and plant productivity under warming climates.

[43] Finally, the results of this study will improve our understanding of the interactive role of the biosphere with the atmosphere. They can be used to verify dynamic vegetation models such as the Dynamic Global Vegetation Models (DGVMs). Although substantial improvements have been made to the DGVMs with regard to representing the dynamics of the vegetation structure and its composition, one of the critical challenges has been a realistic representation of the seasonal evolution of vegetation (*Myoung et al*., 2011; *Richardson et al*., 2012). The ability of vegetation models to capture the dominant inter-annual modes such as the EOF modes and to determine the influences of the meteorological factors can be tested. Such simulations would shed light on a longstanding issue for the scientific community: climate-biosphere interaction and the contribution of plants to the carbon cycle.

[44] **Acknowledgments.** This work was supported by the Basic Science Research Program through the National Foundation of Korea (NRF), funded by the Ministry of Education, Science and Technology (2012-0000857), and the Korea Meteorological Administration Research and Development Program under grant CATER 2012-3064. The authors would like to thank anonymous reviewers for their insightful comments on an earlier draft of this article.

References

Arora, V. (2002), Modeling vegetation as a dynamic component in soil-vegetation-atmosphere transfer schemes and hydrological models, *Rev. Geophys.*, *40*, p.1006.

Brown, M. E., and K. M. de Beurs (2008), Evaluation of multi-sensor semi-arid crop season parameters based on NDVI and rainfall, *Remote Sens. Environ.*, *112*, 2261–2271.

Chandrasekar, K., M. V. R. Sesha Sai, A. T. Jeyaseelan (2006), (Ed- depending on the journal, '*et al*.' is either unacceptable or may only be used after the first 6 authors have been listed) Vegetation response to rainfall as monitored by NOAA–AVHRR, *Curr. Sci.*, *91*, 1626–1633.

Dalezios, N., A. Loukas, and D. Bampzelis (2002), Assessment of NDVI and agrometeorological indices for major crops in central Greece, *Phys. Chem. Earth*, *27*, 1025–1029.

Denman, K. L., et al. (2007), Couplings between changes in the climate system and biogeochemistry. Climate Change 2007: The Physical Science Basis. Contribution of Working Group I to the Fourth Assessment Report of the Intergovernmental Panel on Climate Change, 500–587.

Dickinson, R. E., A. Henderson-Sellers, P. J. Kennedy, and M. F. Wilson (1986), Biosphere-atmosphere transfer scheme (BATS) for the NCAR CCM. NCAR Res., Boulder, CO, NCAR/TN-275-STR.

Foley, J. A., I. C. Prentice, N. Ramankutty, S. Levis, D. Pollard, S. Sitch, and A. Haxeltine (1996), An integrated biosphere model of land surface processes, terrestrial carbon balance, and vegetation dynamics, *Glob. Biogeochem. Cy.*, *10*, 603–628.

Funk, C. C., and M. E. Brown (2006), Intra-seasonal NDVI change projections in semi-arid Africa, *Remote Sens. Environ.*, *101*, 249–256.

Ganguly, S., M. S. Schull, A. Samanta, et al. (2008), Generating vegetation leaf area index earth system data records from multiple sensors. Part 1: Theory, *Remote Sens. Environ.*, *112*, 4333–4343.

Grantz, D. G. (1990), Plant response to atmospheric humidity, *Plant Cell Environ.*, *13*, 667–679.

Hopkins, W. G. (1999), Introduction to plant physiology, Wiley, New York, 469.

Hu, J., D. J. P. Moore, S. P. Burns, and R. K. Monson (2010), Longer growing seasons lead to less carbon sequestration by a subalpine forest, *Glob. Change Biol.*, *16*, 771–783.

Huete, A. R., K. Didan, Y. E. Shimabukuro, et al. (2006), Amazon rainforests green-up with sunlight in the dry season, *Geophys. Res. Lett.*, *33*, L06405, doi:10.1029/2005GL025583.

Ichii, K., A. Kawabata, and Y. Yamaguchi (2002), Global correlation analysis for NDVI and climatic variables and NDVI trends: 1982–1990, *Int. J Remote Sens.*, *23*, 3873–3878.

Jeong, S., C. Ho, H. Gim, and M. E. Brown (2011), Phenology shifts at start vs. end of growing season in temperate vegetation over the Northern Hemisphere for the period 1982–2008, *Glob. Change Biol.*, *17*, 2385–2399.

Körner, C. (1995), Leaf diffusive conductances in the major vegetation types of the globe. Ecophysiology of Photosynthesis, 463–490, Springer, New York.

Koster, R. D., et al. (2004), Regions of strong coupling between soil moisture and precipitation, *Science*, *305*, 1138–1140.

Mu, Q., M. Zhao, F. A. Heinsch, M. Liu, H. Tian, and S. W. Running (2007), Evaluating water stress controls on primary production in biogeochemical and remote sensing based models, *J. Geophys. Res.*, *112*, G01012, doi:10.1029/2006JG000179.

Myneni, R. B., R. R. Nemani, and S. W. Running (1997), Algorithm for the estimation of global land cover, on radiative transfer models, *IEEE Trans. Geosc. Remote Sens.*, *35*, 1380–1393.

Myneni, R. B., W. Z. Yang, R. R Nemani, et al. (2007), Large seasonal swings in leaf area of Amazon rainforests, *Proc. Natl. Acad. Sci.*, *104*, 4820–4823.

Myoung, B., and Y. Deng (2009), Interannual variability of the cyclonic activity along the U.S. Pacific Coast: Influences on the characteristics of winter precipitation in the Western United States, *J. Climate*, *22*, 5732–5747.

Myoung, B., and J. W. Nielsen-Gammon (2010a), The convective instability pathway to warm season drought in Texas. Part I: The role of convective inhibition and its modulation by soil moisture, *J. Climate*, *23*, 4474–4488.

Myoung, B., and J. W. Nielsen-Gammon (2010b), The convective instability pathway to warm season drought in Texas. Part II: Free-tropospheric modulation of convective inhibition, *J. Climate*, *23*, 4474–4488.

Myoung, B., Y. S. Choi, and S. K. Park (2011), A review on vegetation models and applicability to climate simulations at regional scale Asia-Pac, *J. Atmos. Sci.*, *47*, 463–475.

Nemani R, C. D. Keeling, H. Hashimoto, W. Jolly, S. Piper, C. Tucker, R. Myneni, and S. Running (2003), Climate-driven increases in global terrestrial net primary production from 1982 to 1999, *Science*, *300*, 1560–1563.

Nezlin, N. P., A. G. Kostianoy, and B. L. Li (2005), Inter-annual variability and interaction of remote-sensed vegetation index and atmospheric precipitation in the Aral Sea region, *J. Arid Environ.*, *62*, 677–700.

Pettorelli, N., et al. (2005), Using the satellite-derived NDVI to assess ecological responses to environmental change, *Trends Ecol. Evol.*, *20*, 503–510.

Piao, S. L., J. Y. Fang, L. M. Zhou, Q. Guo, M. Henderson, W. Ji, Y. Li, and S. Tao (2003), Interannual variations of monthly and seasonal normalized difference vegetation index (NDVI) in China from 1982 to 1999, *J. Geophys. Res.*, *108*, (4401) doi:10.1029/2002JD002848.

Pielke, R. A., R. Avissar Sr, M. Raupach, A. J. Dolman, X. Zeng, and A. S. Denning (1998), Interactions between the atmosphere and terrestrial ecosystems: influence on weather and climate, *Glob. Change Biol.*, *4*, 461–475.

Prentice, C., M. Heimann, and S. Sitch (2000), The carbon balance of the terrestrial biosphere: Ecosystem models and atmospheric observations, *Ecol. Appl.*, *10*. 1553–1573.

Priesendorfer, R. W. (1988), Principle Component Analysis in Meteorology and Oceanography, Elsevier Science, New York, 425.

Quillet, A., C. Peng, and M. Garneau (2010), Toward dynamic global vegetation models for simulating vegetation–climate interactions and feedbacks: recent developments, limitations, and future challenges, *Environ. Rev.*, *18*, 333–353.

Rastetter, E. B., A. W. King, B. J. Cosby, G. M. Hornberger, R. V. O'Neill, and J.E. Hobbie (1992), Aggregating fine-scale ecological knowledge to model coarser-scale attributes of ecosystems, *Ecol. Appl.*, *2*, 55–70.

Reed B. C., M. D. Schwartz, and X. Xiao (2009), Remote sensing phenology: status and the way forward. In Phenology of ecosystem processes (ed. Noormets A.), Springer. 231–246.

Richard, Y., and I. Poccard (1998), A statistical study of NDVI sensitivity to seasonal and interannual rainfall variations in Southern Africa, *Int. J. Remote Sens.*, *19*, 2907–2920.

Richardson A. D., et al. (2010), Influence of spring and autumn phenological transitions on forest ecosystem productivity, *Phil. Trans. R. Soc. B 365*, 3227–3246.

Richardson, A. D., et al. (2012), Terrestrial biosphere models need better representation of vegetation phenology: results from the North American Carbon Program Site Synthesis, *Glob. Change Biol.*, *18*, 566–584.

Sacks,W. J., D. S. Schimel, and R. K. Monson (2007), Coupling between carbon cycling and climate in a high-elevation, subalpine forest: a model-data fusion analysis, *Oecologia*, *151*, 54–68.

Sarkar, S., and M. Kafatos (2004), Interannual variability of vegetation over the Indian sub-continent and its relation to the different meteorological parameters, *Remote Sens. Environ.*, *90*, 268–280.

Sellers, P. J., R. E. Dickinson, A. Randall, A. K. Betts, F. G. Hall, J. A. Berry, G. J. Collatz, A. S. Denning, H. A. Mooney, C. A. Nobre, N. Sato, C. B. Field, and A. Henderson-Sellers (1997), Modeling the exchanges of energy, water, and carbon between continents and the atmosphere, *Science*, *275*, 502–509.

Sharon, E. N., M. L. Davenport, and A. R. Malo (1990), A comparison of the vegetation response to rainfall in the Sahel and East Africa, using normalized difference vegetation index from NOAA AVHRR, *Clim. Chang.*, *17*, 209–241.

Studer, S., C. Appenzeller, and C. Defila (2005), Inter-annual variability and decadal trends in Alpine spring phenology: a multivariate analysis approach, *Clim Change*, *73*, 395–414

Studer, S., R. Stöckli, C. Appenzeller, and P. L. Vidale (2007), A comparative study of satellite and ground-based phenology, *Int. J. Biometeorol. 51*, 405–414.

Vesala, T., et al. (2009), Autumn warming and carbon balance of a boreal Scots pine forest in Southern Finland, *Biogeosci. Discuss. 6*, 7053–7081.

Wang, J., P. M. Rich, and K. P. Price (2003), Temporal responses of NDVI to precipitation and temperature in the central Great Plains, USA, *Int. J. Remote Sens.*, *24*, 2345–2364.

Wang, W., B. T. Anderson, N. Phillips, R. K. Kaufmann, C. Potter, and R. B. Myneni (2006) Feedbacks of vegetation on summertime climate variability over the North American grasslands. Part I: statistical analysis, *Earth Interactions*, *10*, 1–27.